

# Design and Experimental Research of an Automatic Wolfberry Harvesting Robot using Vibration

1<sup>st</sup> Muhammad Mubashir Niaz  
School of Mechanical Engineering  
Southeast University  
Nanjing, China  
mubashirniaz27@gmail.com

4<sup>th</sup> Mohammad Abbas Baig  
School of Mechanical Engineering  
Southeast University  
Nanjing, China  
murcielo.goda@gmail.com

2<sup>nd</sup> Liang Han\*(Corresponding author)  
School of Mechanical Engineering  
Southeast University  
Nanjing, China  
melhan@seu.edu.cn

5<sup>th</sup> Danaish  
School of Mechanical Engineering  
Southeast University  
Nanjing, China  
danaish2013@gmail.com

3<sup>rd</sup> Rui Zeng  
School of Mechanical Engineering  
Southeast University  
Nanjing, China  
220200242@seu.edu.cn  
6<sup>th</sup> Muhammad Sibtain  
School of Mechanical Engineering  
Southeast University  
Nanjing, China  
enr.msibtain114@gmail.com

**Abstract**— With the rapid development of the social economy and the growing in demand for healthy food, the scale of wolfberry planting and the market demand for wolfberry continue to expand. The wolfberry industry is experiencing vigorous growth. The industry is facing increasingly prominent problems such as high cost, difficulty in picking, and low efficiency, which are restricting its growth. We have thoroughly investigated the current research status of the wolfberry industry and compiled a summary of the advantages and disadvantages of various berry picking devices. To solve the above problems, we developed an automatic harvesting robot. The overall design scheme includes the drone with machine vision recognition technology the vibrator, collector, and Rail guided vehicle (RGV). Results from robot vibration experiments and slow-motion shedding experiment confirm the effectiveness of the vibration induced fruit harvesting process.

**Keywords**—Wolfberry, Automatic harvesting, Vibration, field Experiment

## I. INTRODUCTION

In response to growing consumer interest in both domestic and international markets, wolfberry cultivation has been underway for the last few decades. Due to the existing market demand for this super-fruit widely used in Asian traditional medicine and promoted for its numerous health benefits [1]. This crop required more advanced agricultural practices, particularly in the field of harvesting. Currently, the existing harvesting method is ineffective, both in terms of efficiency and costs, as it is primarily manual, and such an approach has become unsustainable given the heightened demand for this fruit and the increasing shortage of agricultural workers [2],[3].

Mechanical methods, such as use of vibration and brush, or air suction, have been created before; however, each of those has certain significant disadvantages. For example, the air-suction method has the potential to increase efficiency, but yet it may harm the ripe fruits, and vibration-based techniques may harm the ripe fruits as well as leaves and tree [4]. Therefore, there is a need to find a solution that boosts process efficiency, ensures gentle handling of the fruits, and ensures the high quality of fruits. This research will address this gap by presenting a mechanized harvesting system specifically for wolfberries. This approach will include advanced robot based on the farm's

planting specifications and cover problems in the harvest process.

The concept of automatic harvesting on wolfberry farms is combined with a unique machine vision recognition technology that can automatically identify ripe fruits. Furthermore, the proposed new system should optimize the crop's physical layout and adapt to mechanized harvesting

## II. OVERALL SYSTEM FRAMEWORK

### A. Drone station

The Drone IoT unit consists of a sensing system, a ground-based station, and cloud data [5]. Among them, the Drone sensing system includes a binocular camera, and a humidity sensor. as shown in Fig. 1. The visual sensor identifies the maturity of fruits in the wolfberry garden based on their color. A binocular camera is used for the three-dimensional data acquisition of the wolfberry garden; humidity sensors are used to detect the atmospheric environment, such as air precipitation [6]. The drone IOT unit provides users with remote mobile information transmission and control solutions. The front-end is the mobile interface, which provides information about the plant's growth, harvesting times, and harvesting situation. The cloud database connects to the back-end, enabling the user to access data at any time by entering their system account password.

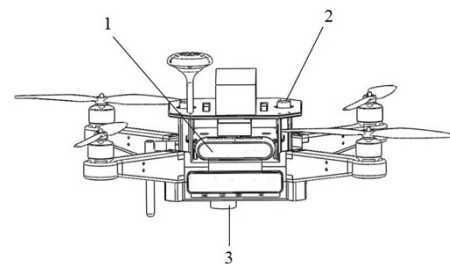


Fig. 1. The schematic diagram of Drone sensing system  
1-Binocular camera;2-Humidity sensor;3-Vision camera

The wolfberry harvesting robot microprocessor receives the input harvesting signal from the wolfberry plant and uses it to control the operation of the harvest device during excitation

harvesting, as shown in Fig. 2. Once harvesting is complete, the robot returns to the storage warehouse for sorting and delivery.

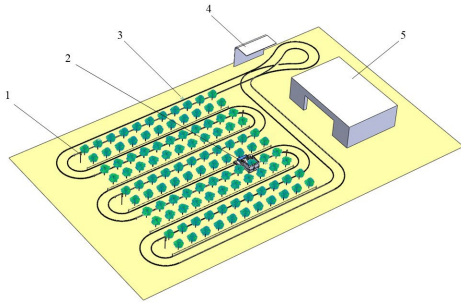


Fig. 2. The schematic diagram for automatic harvesting device

- 1: Lights; 2-Automatic wolfberry Picking device; 3-Drone; 4-Charging post; 5-Wolfberry storage bin

### B. System overall composition

This paper proposes a wolfberry harvesting robot to address current issues in wolfberry picking and evaluate the benefits and drawbacks of different types of harvesting machinery, recognizing that Plant specification plays a crucial role in creating an agricultural visualization map that facilitates a smooth automatic harvesting process. To achieve this, we developed a data system to meet the demands of wolfberry farms and ensure planting feasibility. In the data system, we assign a code to each plot of land, regardless of its size, and mark a consecutive tree number, associating it with the system's serial number, which helps us identify ripe fruit during harvesting [7]. The wolfberry planting area spans 1.5 acres with a row spacing of 2.5 m between columns and a plant spacing of 1.5 m, one acre of land can accommodate 178 wolfberry Plants.

This system is characterized by its mechanical automation operation, high quality and efficient harvesting, minimal damage to trees, and commitment to environmental sustainability. The structure of the automatic harvesting robot mainly includes a vibrator, collector, RGV, conveyor belt, fruit box, and its specific workflow, as shown in Fig. 3. Once the Drone visual camera captures a reddish area in the wolfberry garden, the Drone IOT system gathers and stores the geographic position of the mature wolfberry area. It then transmits this data to the computer. The computer compares the location's latitude and longitude with those of the wolfberry garden, determines the serial number of the wolfberry plant within this boundary, and use the CAN bus to communicate with the hardware in real time to control the automatic wolfberry harvesting robot start-up.

When the wolfberry automatic harvest robot travels to a specific wolfberry plant according to its serial number the magnetic Hall sensor placed on the robot stops it and activates control process of the collector. The vibrator begins to apply vibration force to the wolfberry plant's trunk. After the vibrating process, the device effectively collects ripe wolfberry fruits and transfers them to the backup fruit box [8]. The robot immediately moves on to the next wolfberry plant, repeating the cycle until it has finished harvesting the designated area of wolfberry plants. When the harvested weight reaches the demand value, the wolfberry harvesting robot will go to the wolfberry storage

warehouse for unloading. That process finished in eight minutes. After unloading, it waits for the next instructions from the operator to continue harvesting according to the serial number or go to any specific plot for harvesting operations.

When the robot power drops below 15%, it will trigger the charging interrupt input 1, stop the current harvesting operation, and travel to the charging port for charging. When the drone humidity sensor detects the rainstorms, thunder, and lightning above the wolfberry garden, it will also trigger interrupt input 2 to stop the automatic harvesting device and move to the charging port for shelter from the rain and to wait. When the power reaches 100% and the weather clears, the system will restart the robot for harvesting; If the harvesting robot malfunctions or encounters other faults, the alarm system will be activated to remind management personnel to maintain it.

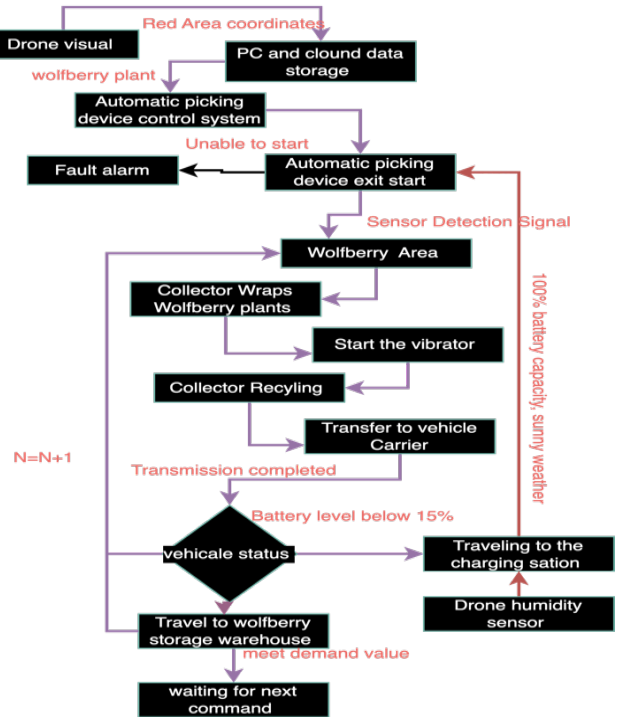


Fig. 3. Flowchart for Wolfberry harvesting robot

### III. MECHANICAL MODULE DESIGN

The combination of the aforementioned programs allows us to design the overall layout of the wolfberry harvesting robot, as illustrated in Fig. 4.[9].The robot primarily consists of a vibrator, collector, RGV, and removable power supply, all of which work together to successfully harvest the wolfberry fruits.

With high standardization requirements for wolfberry plantations and low initial construction costs, this robot design makes it suitable for long-term use in harvesting. Considering the significant variations in the current wolfberry planting land environment, planting size areas, manufacturing cost of the fully automated device, and other important factors, we can create an automatic harvesting robot with human assistance that can not only adapt to the uneven wolfberry planting land environment but also expedite its manufacture.

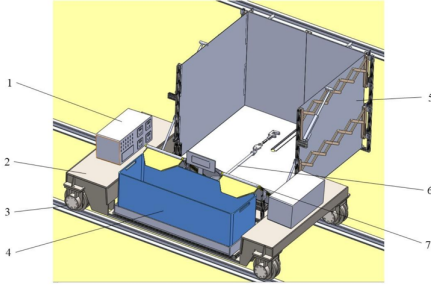


Fig. 4. The schematic diagram for automatic harvesting device

1-Removable power source; 2-Car carrier; 3-RGV; 4-Fruit box;  
5-Collector; 6-Vibrator; 7-Conveyor belt

#### A. Vibrator structure design

The vibrator consists of a DC motor, drive shaft, gear system, crank linkage mechanism, clamping mechanism, and ratchet mechanism. As shown in Fig. 5. A coupling connects the output shaft to the drive shaft, while the gearing system drives the crank linkage. The end clamping mechanism fits into a U-shaped groove around the wolfberry tree trunk, allowing the reciprocating motion of the crank linkage mechanism to induce vibrations in the plant. The vibrator imposes a variable frequency of harmonic excitation to harvest wolfberry fruit at different maturity levels.[10]. The vibrator's total length of 1.6 m allows for adaptability to the row spacing size of the wolfberry garden.

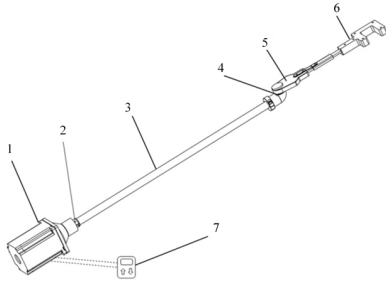


Fig. 5. Vibrator Structure

1- DC motor; 2 - Coupling; 3 - Transfer shaft; 4 - Ratchet; 5 -Internal gear tooth system; 6 - Clamping mechanism

#### B. Rectangular body collector

This paper proposes a new type of collection method: a rectangular body collector. The principle of the rectangular body collector is to use the two sides of the canvas and the back canvas to effectively shield the vibration of the splash of berries ensuring that they fall on to the bottom canvas. as shown in Fig. 6. This setup allows for the recovery of the berries after they fall. The back of the canvas extends beyond the wolfberry plant, wrapping around it to form a rectangular body space. The vibrator, which acts on the plant stem, completes the fruit vibration.

When the harvesting process is complete the rectangular body collector can efficiently gather wolfberry fruit, utilize the wolfberry plant's row spacing, and adapt to the uneven harvesting conditions of wolfberry planting land.

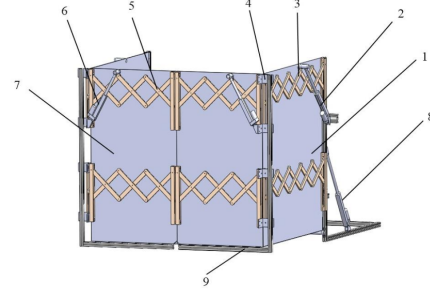


Fig. 6. Rectangular body collector

1-Both sides canvas; 2-Both sides motorized actuator; 3-Both sides shear frame; 4-Right angle piece; 5-Back shear frame;6-Back electric actuator; 7-Back canvas; 8-Flip electric actuator; 9-Aluminum frame.

### IV. EXPERIMENTAL STUDY

#### A. Measurement of the elastic modulus

For the experiment, we selected six branches, each with an average diameter of 5 mm, from the four levels of the main branches: primary branch, secondary branch, fruit branch, and main branch of the tree, using the principle of the three-point bending test. We set the span to 200 mm and measured the average deflection of the branches at 40.01 mm under a load of 10 N. We measure the modulus of elasticity of fresh branches using the three-point bending test formula.

$$E = \frac{4l^3}{3\pi d^4} \frac{P}{Y} \quad (1)$$

Where,  $E$  - flexural modulus of elasticity, MPa;  $l$  - pivot span, mm;  $d$  - average diameter of branches, mm;  $P$  - concentrated load, N;  $Y$  - deflection mm.

According to equation (2), the average flexural modulus of elasticity of the four levels of primary branches of the wolfberry plant can be obtained as.

$$E = \frac{4 \times 200^3 \times 10}{3 \times \pi \times 5^4 \times 40.01} = 1357.783 \text{MPa} \quad (2)$$

In the wolfberry plant branches, at the end of the four main branches compared with other levels of the main branches and the trunk, more flexible, easy to deform, so the modulus of elasticity is relatively small, and the value of the modulus of elasticity of the main branches of the wolfberry plant can often reach 6.9Gpa.

#### B. Measurement of mass of wolfberry fruits

The quality of the fruit is very important to study and analyze before the vibration of wolfberries. In this experiment, we used an LQ-10003 electronic scale to determine the fruit's weight. Its graduation value is 0.001 g, and features tare, calibration, multi-unit conversion, and other functions. The experimental method involves screening 100 pieces of ripe, semi-mature, and green fruits, measuring their respective masses, and then calculating the average value of the measurement data to determine the average mass of ripe, semi-mature, and green fruits.

The average mass of ripe, semi-mature, and green fruits was 0.124 g, 0.680 g, and 0.222 g, respectively.

### C. Vibration experiment system construction

The experiment took place in inner Mongolia was completed over two days on different trees to ensure better results. Fig. 7. Shows the experimental arrangement. The goal of this experiment was to investigate the evacuated, layered type of wolfberry plant of a certain size and determine the optimal frequency range for an automatic harvesting robot.

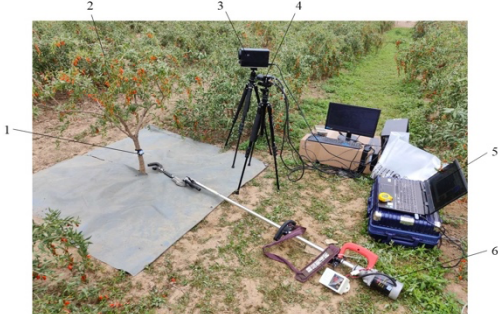


Fig. 7. Experimental test on the vibration of wolfberry

1-Gyroscope; 2- WB strain; 3- Light source; 4- High speed camera; 5- Data acquisition system; 6- Vibrator

### D. Analysis of vibration results

As mentioned, the hardware construction of the vibration experiment on the wolfberry plant involved sequentially vibrating six branches at five frequency adjustments: 3.554Hz, 7.108Hz, 10.663Hz, 14.217Hz, and 17.366Hz. This section focused on the vibration characteristics of the plant stem. At the start of the experiment, the relative positions of the acceleration sensor and the clamping mechanism at the end of the vibrator,

were examined in detail. It was discovered that changes in the relative positions between 0 and 60 cm had a smaller impact on the acceleration than changes in the frequency value we found that a change in relative position within the range of 0-60 cm had less effect on the acceleration than a change in frequency, indicating that the overall acceleration of the stem was located at the middle height of the stem.

Therefore, in this experiment, the height of the vibration was selected to be 30cm from the bottom surface of the stem, the acceleration sensor was located close to the vibration position, and the vibration time at each frequency was 10 second, and the data parameters in Tables I. and Tables II. were obtained through data acquisition and experimental calculations. Table 1. contains the x and y components of the acceleration of wolfberry stem, collected by the acceleration sensor at each vibration frequency, while Table II. provides statistics on the fruit drop of wolfberry plants at various vibration frequencies. In this paper, we select the wolfberry plant with the best harvesting effect and a vibration frequency of 14.217 Hz to reflect the overall process of collecting data, as shown in Fig. 8.

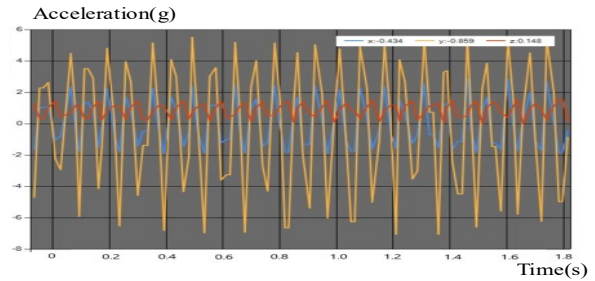


Fig. 8. Acceleration acquisition graph.

TABLE I. ABSOLUTE VALUES OF THE LOWER X, Y COMPONENTS OF THE MAXIMUM ACCELERATION OF WOLFBERRY STEM AT DIFFERENT VIBRATION FREQUENCIES

| Acceleration<br>Plant<br>serial number | 20%RPM      |         | 40%RPM      |         | 60%RPM      |         | 80%RPM      |         | 100%RPM     |         |
|--|-------------|---------|-------------|---------|-------------|---------|-------------|---------|-------------|---------|
|  | $a_{max/g}$ |         | $a_{max/g}$ |         | $a_{max/g}$ |         | $a_{max/g}$ |         | $a_{max/g}$ |         |
|  | $ a_x $     | $ a_y $ | $ a_x $     | $ a_y $ | $ a_x $     | $ a_y $ | $ a_x $     | $ a_y $ | $ a_x $     | $ a_y $ |
| 1                                      | 0.20        | 0.45    | 0.64        | 1.83    | 1.89        | 4.01    | 1.86        | 7.11    | 2.72        | 11.40   |
| 2                                      | 0.09        | 0.47    | 0.42        | 1.90    | 2.00        | 4.10    | 1.77        | 7.21    | 2.42        | 11.63   |
| 3                                      | 0.15        | 0.39    | 0.51        | 1.78    | 1.51        | 3.82    | 1.99        | 7.06    | 3.13        | 11.20   |
| 4                                      | 0.21        | 0.35    | 0.35        | 1.72    | 1.72        | 3.97    | 1.88        | 6.99    | 3.05        | 10.88   |
| 5                                      | 0.20        | 0.38    | 0.34        | 1.63    | 2.27        | 3.59    | 1.83        | 7.00    | 3.04        | 10.58   |
| 6                                      | 0.05        | 0.40    | 0.31        | 1.98    | 1.28        | 3.95    | 1.97        | 7.12    | 2.76        | 11.25   |

TABLE II. THE EFFECT OF VIBRATION ON WOLFBERRY PLANTS AT DIFFERENT FREQUENCIES

| RPM  | Clamping mechanism frequency (Hz) | Vibration amplitude (mm) | Average Maximum Acceleration of Stem (1g) | Average Number of Fruit Drops (pieces) | Fruit Quality    | Leaf and branch drop              |
|------|-----------------------------------|--------------------------|---|--|------------------|-----------------------------------|
| 20%  | 3.554                             | 20                       | 0.448                                     | 4                                      | Fresh            | No drop                           |
| 40%  | 7.108                             | 20                       | 1.917                                     | 24                                     | Fresh            | No drop                           |
| 60%  | 10.663                            | 20                       | 4.244                                     | 148                                    | Fresh            | drop a small amount               |
| 80%  | 14.217                            | 20                       | 7.3227                                    | 204                                    | Fresh            | Drop some leaves.                 |
| 100% | 17.636                            | 20                       | 11.520                                    | 50                                     | Little scratches | Lots of leaf loss 1 branch broken |

## V. CONCLUSION

This paper discusses the harvesting needs of wolfberry farming in Inner Mongolia, addressing current challenges such as high costs, low efficiency, poor quality, and labor-intensive manual picking. This paper proposes an automatic solution for wolfberry harvesting. Our system uses a drone's machine vision recognition technology to pinpoint ripe berry locations. The Robot four constituent parts the vibrator, collector, and RGV carrier collaboratively complete the harvesting, reduce expenses, and increase profit. Our automatic harvesting robot enhances the speed and efficiency of fruit harvesting while simultaneously preventing excessive damage to plants and the environment.

We did tests in the field to find out the effective frequency range of vibration and the resulting acceleration of the wolfberry plant stem at each frequency. We also checked the quality of the fruit after the vibration. Using a high-speed camera, we recorded the slow motion of the fruit shedding to confirm the authenticity of the vibration-induced fruit drop. Our experimental study results indicate that 95% of the fruits vibrated off have fresh skin with no signs of damage.

## REFERENCES

- [1] Y. Ma, W. Zhang, W. S. Qureshi, C. Gao, C. Zhang, and W. Li, "Autonomous navigation for a wolfberry picking robot using visual cues and fuzzy control," *Inf. Process. Agric.*, vol. 8, no. 1, pp. 15–26, Mar. 2021.
- [2] W. Jinpeng, M. Song, X. Hongru, Z. Ying, and Z. Hongping, "Research on Mechanized Harvesting Methods of Lycium barbarum Fruit," *IFAC-Pap.*, vol. 51, no. 17, pp. 223–226, 2018.
- [3] Y. Chen, J. Zhao, G. Hu, and J. Chen, "Design and Testing of a Pneumatic Oscillating Chinese Wolfberry Harvester," *Horticulturae*, vol. 7, no. 8, p. 214, Jul. 2021.
- [4] J. Zhao et al., "Modal Analysis and Experiment of a Lycium barbarum L. Shrub for Efficient Vibration Harvesting of Fruit," *Agriculture*, vol. 11, no. 6, p. 519, Jun. 2021.
- [5] J. Shi, Y. Bai, Z. Diao, J. Zhou, X. Yao, and B. Zhang, "Row Detection BASED Navigation and Guidance for Agricultural Robots and Autonomous Vehicles in Row-Crop Fields: Methods and Applications," *Agronomy*, vol. 13, no. 7, p. 1780, Jun. 2023.
- [6] R. Ramin Shamshiri et al., "Research and development in agricultural robotics: A perspective of digital farming," *Int. J. Agric. Biol. Eng.*, vol. 11, no. 4, pp. 1–11, 2018.
- [7] F. Ma, L. Li, Y. Wang, P. Li, and C. Zhu, "BIOMECHANICAL PROPERTIES OF WOLFBERRY PLANT ORGANS," *Eng. Agric.*, vol. 40, no. 2, pp. 162–176, Apr. 2020.
- [8] A. Mohanty, S. Parida, R. K. Behera, and T. Roy, "Vibration energy harvesting: A review," *J. Adv. Dielectr.*, vol. 09, no. 04, p. 1930001, Aug. 2019.
- [9] S. Wei, J. Hao, S. Liu, and X. Zhang, "Design of Chinese Wolfberry Picking Robot System," in *2021 2nd International Conference on Artificial Intelligence and Information Systems*, Chongqing China: ACM, May 2021.
- [10] K. Zhang, K. Lammers, P. Chu, Z. Li, and R. Lu, "System design and control of an apple harvesting robot," *Mechatronics*, vol. 79, p. 102644, Nov. 2021.

The sensor divides the acceleration data into three axes, x,y, and z. The z-axis aligns with the direction of gravity and fluctuating within 1 g, while the y-axis aligns with the main vibration direction. From the figure, it is evident that the collected curve exhibits a vibration frequency of approximately 14.2 Hz, which match the frequency applied by the vibrator.

In addition, there is an asymmetry between the upper and lower curves, which is due to the gap of 5–10 mm between the clamping width of the vibrator and the diameter of the trunk. The gap results in higher acceleration peaks in the upper half of the y-axis compared to the lower half. The values in the upper right corner of the graph represent the acceleration values of each axis around 1.9 seconds. The values at the rightmost end of the curve, reflecting the real-time acceleration acquisition. Table II. shows that the current effective vibration frequency for harvesting wolfberry plants ranges from 10.663 Hz to 14.217 Hz. In addition, Furthermore, the simulated intrinsic frequency under free vibration of wolfberry branches and single-layer wolfberry plants was 13.547 Hz, which falls within the effective vibration frequency range identified in the experiment.

As shown in Fig. 9.the quality acceptance of the vibrated fruits at each frequency shows that in a short time, more than 95% of the fruits vibrated off the skin are shiny and fresh, with no signs of damage. The wolfberry fruit's head is a perfect point for a high-quality harvest.



Fig. 9. Fruit falls at each frequency due to vibrational effects

### C. Slow-motion analysis of fruit shedding

We captured the slow-motion shedding of wolfberry fruit by setting a high-speed camera to shoot at 3000 frames per second from a height of 1 meter. This setup allowed us to fully observe the detailed vibration process of the wolfberry branches, fruits, and leaves. Given that wolfberry plant vibration falls within the low-frequency range, we also used a smartphone slow motion feature at 480 frames per second for additional viewpoints. The experimental results show that both the high-speed camera and the slow-motion camera of the cell phone captured the entire process of the wolfberry fruits from different angles, as shown in Fig. 10. and Fig. 11.

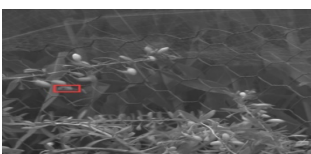


Fig. 10. A slow-motion image from a high-speed camera



Fig. 11. A slow-motion image from a mobile phone camera